Application note

Current sensing in BLDC motor application

Introduction

The brushless DC motor is very popular in industrial automation, automotive, medical, and health care applications due to its high reliability and lifespan. As it becomes increasingly accessible to cost-sensitive markets, the focus now shifts to electronics that can interface with BLDC motors to maximize efficiency. Fast and precise current sensing becomes key to ensure reliable feedback on speed, angle, and rotation direction.

This application note introduces some different techniques for current sensing, with a focus on the inline phase current. It requires dedicated current sensing ICs, which are able to work with common-mode significantly higher than the power supply, and deliver good and fast responses to fast common-mode step variation.

This document addresses current measurement in BLDC motors for a three-phase topology described in a simplified schematic in Figure 2.

1 How it works

Before addressing the current measurement of a BLDC motor, it is useful to understand the functional principles. BLDC motors are “synchronous” devices, which means that stator flux (and thus motor phase currents) must be kept synchronous with the rotor position, which, as a result, must always be known.

In order to make the motor run, the magnetic field generated by the stator must be checked by considering the current flowing into the motor phase. Current feedback has to be as fast and precise as possible in order to control the motor phase current.

Rotor position and speed have to be known in order to achieve synchronization. The BLDC driver powers the stator winding sequentially, generating an electric field which in turn makes the rotor run. In order to guarantee efficient operation, the winding must be powered at the right time. The schematic below describes a 6-step mode drive.

Figure 1. Current in winding A, B, C

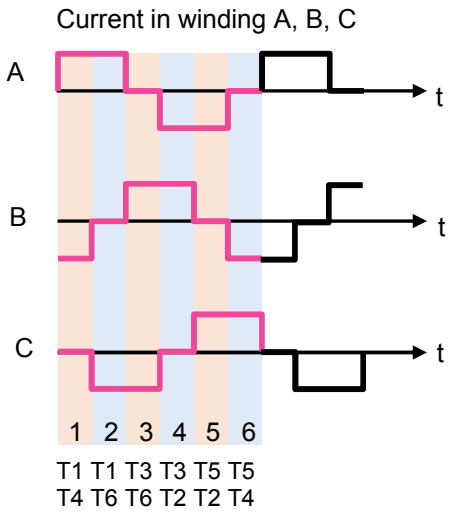

Figure 2. 6-step mode drive

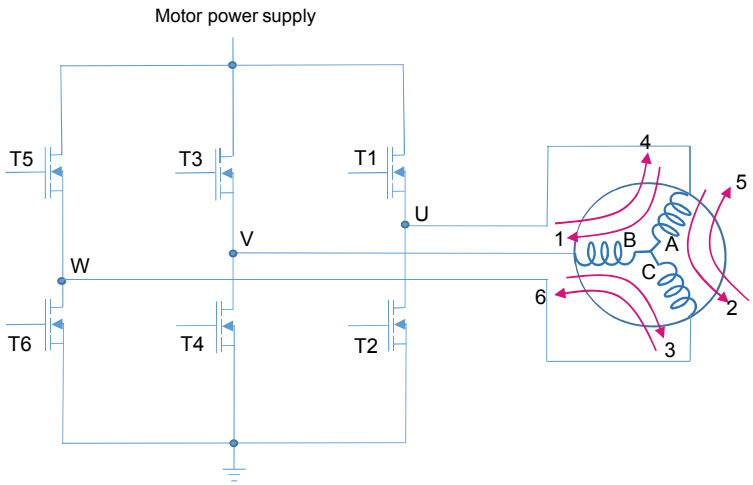

During one electrical cycle, there is always one winding biased in one direction and another in the other direction.

In the first step, the transistors T1 and T4 are closed, so that current flows through winding A and B. In this manner, the rotor moves to 60 °. In the next step, the transistors T1 and T6 are closed. The current flows through the winding A and C and the rotor moves to more than 60 °.

Some BDLC motors have a Hall sensor embedded in the motor. The main function of the Hall sensor is to know the rotor position to be able to energize the right winding for a good commutation sequence.

In order to simplify motor construction, or for application working in dusty and oily environments, some BLDC motors are sensorless. Therefore, no Hall sensor is integrated to detect the motor position.

In this case, other techniques can be used to provide feedback information about the motor. One of them uses the back electromotive force (back-EMF) effect. This technique uses the zero-crossing of the BEMF to determine the rotor position.

Back-EMF is a voltage that occurs in the opposite direction to current flow as a result of the motor coils moving in a magnetic field, and it is proportional to the speed of the rotor.

One of the main drawbacks of back-EMF measurement is when the motor runs at low speed or stops, and no information is provided to determine the motor position.

Maximum efficiency is achieved if the commutation between two consecutive steps is performed only when the rotor is in the right spatial position, which occurs when the back-EMF signal and the phase current are synchronized.

Figure 3. Correlation between current and back-EMF

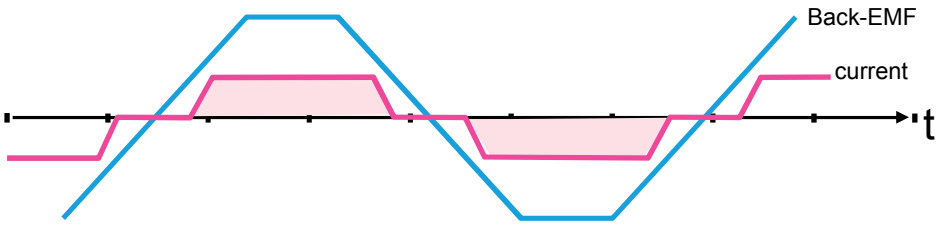

If current and back-EMF are not in phase, then the BLDC does not run efficiently or stops. Therefore, the current in such applications has to be sensed.

Vector control, also called field-oriented control (FOC) is another algorithm used to check this kind of motor. It is a mathematical technique used to achieve decoupled control of the flux and torque in a three-phase machine. It is a high-end technique, but it is becoming increasingly popular. This kind of algorithm is based on a fine control of the motor currents, which have to be sensed in real time and with sufficient accuracy to achieve optimized motor control. There are four different techniques to monitor the current in a BDLC application, each of them with different advantages and disadvantages.

1.1 Low-side global current sensing

The simplest topology is described in the figure below. It is a global low-side current sensing method. The main advantage of this technique is that the common-mode voltage is close to ground, allowing for a wide range of low voltage op amps to be used. In addition, the low cost makes this technique a very interesting solution.

Figure 4. Low-side global current sensing configuration

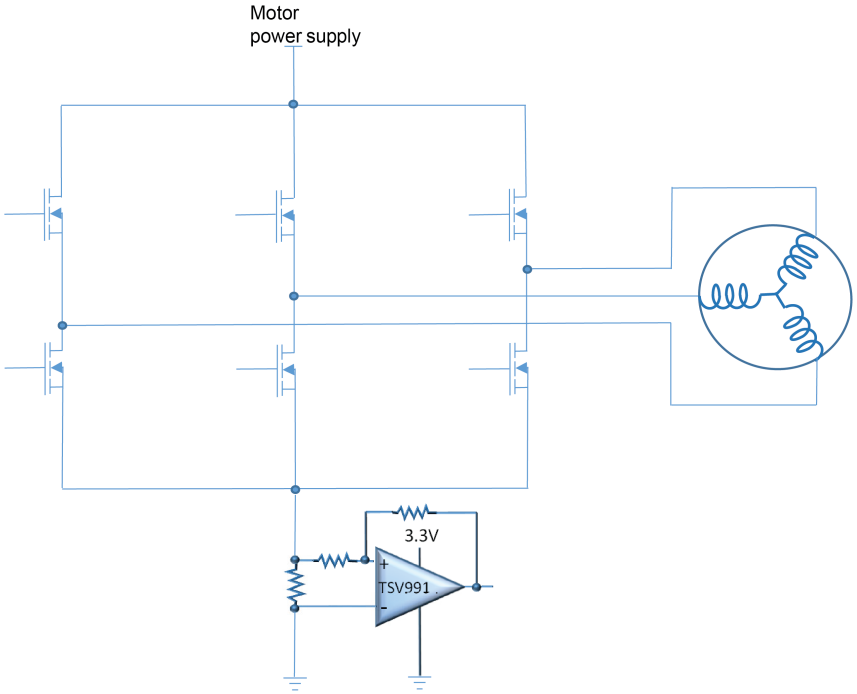

It is generally chosen when a certain fault must be detected. As it is a low-side technique, it cannot allow a short-circuit to ground detection and thus motor failure. Moreover, the measured current does not necessarily match the actual current flowing through the motor. In order to identify the phase current in this location, a very high slew rate op amp is required, as well as a very complex algorithm to handle this information, which is in contrast with the expected low-cost solution. The TSV771, a high-bandwidth and low-offset op amp, can be used for this configuration. In addition, the TSV991 can be used with a minimum gain of 4 for applications with a power supply V_{CC} lower than 5 V.

1.2 Low-side current sensing in each leg of the current driver

Comparing the 3-shunt low-side technique with the previous version allows a better estimation of the phase current flowing into the motor, even if it is not an exact equivalent. The low-side configuration allows the use of low-power op amp, as the common-mode is close to ground. However, this current measurement is sensitive to ground variation and does not detect short circuits to ground. This topology is largely used in FOC.

Figure 5. Low-side current sensing in each leg of the current driver

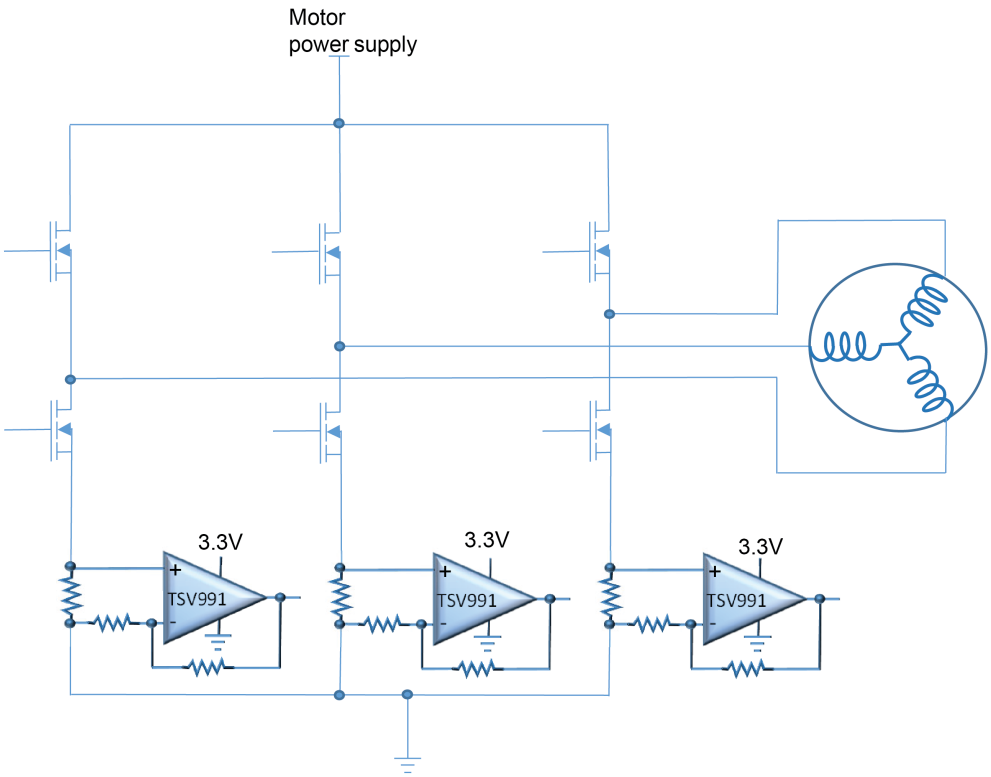

The third current measurement branch is optional and can be calculated in the controller. The TSV991 can be used with a minimum gain of 4 for applications with a power supply V_{CC} in the range of 2.5 V to 5.5 V.

This topology is described in detail in the AN4076.

1.3 High-side current sensing

Unlike the previous configurations, this one detects the short-circuit to ground, and since it is placed close to the supply, the current measurement is not sensitive to ground disturbance. This configuration needs a special op amp that can work with high-voltage common-mode inputs. In this configuration, the input common-mode voltage is quite stable, and the amplifier does not require any special care regarding fast common-mode voltage variation.

In this case, nevertheless, the current which is measured does not match the phase current flowing into the motor exactly.

Figure 6. High-side current sensing

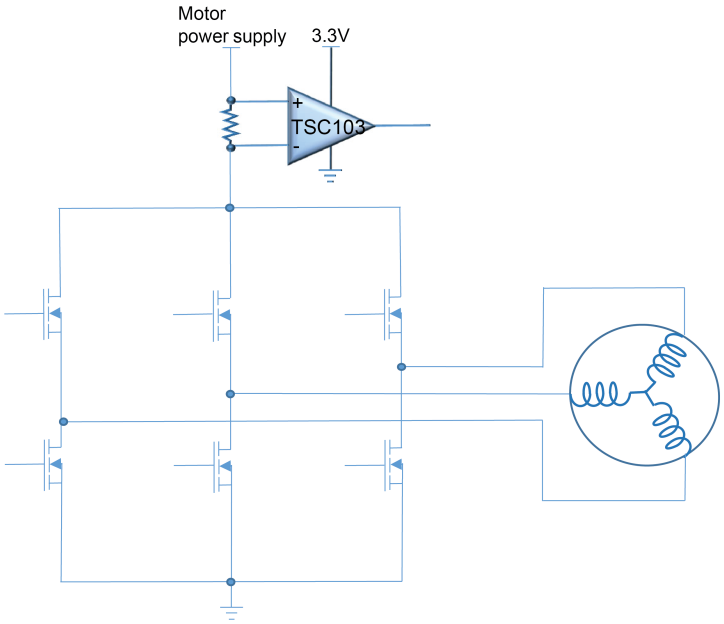

The TSC103 can be used in a high-side current sensing.

By combining the topology depicted in Figure 6 and Figure 4, the leakage is detected by calculating the difference between the low-side and the high-side current measurement.

1.4 Inline phase current

The configuration described in Figure 7 is the best method to precisely determine the phase current flowing into the motor.

This current measurement offers the best information that can be used in feedback motor control to optimize the motor performance, because the current is monitored continuously.

As the shunt resistance is placed directly in line with the PWM driver, a dedicated current sensor is used, which rejects fast common-mode variations.

The input pins of the current sensor can be subjected to several tens of volt in a few nanoseconds, depending on the motor to drive. The current sensor should be able to reject this variation, and limit unwanted disturbance on the output as much as possible.

Figure 7. Inline phase current sensing

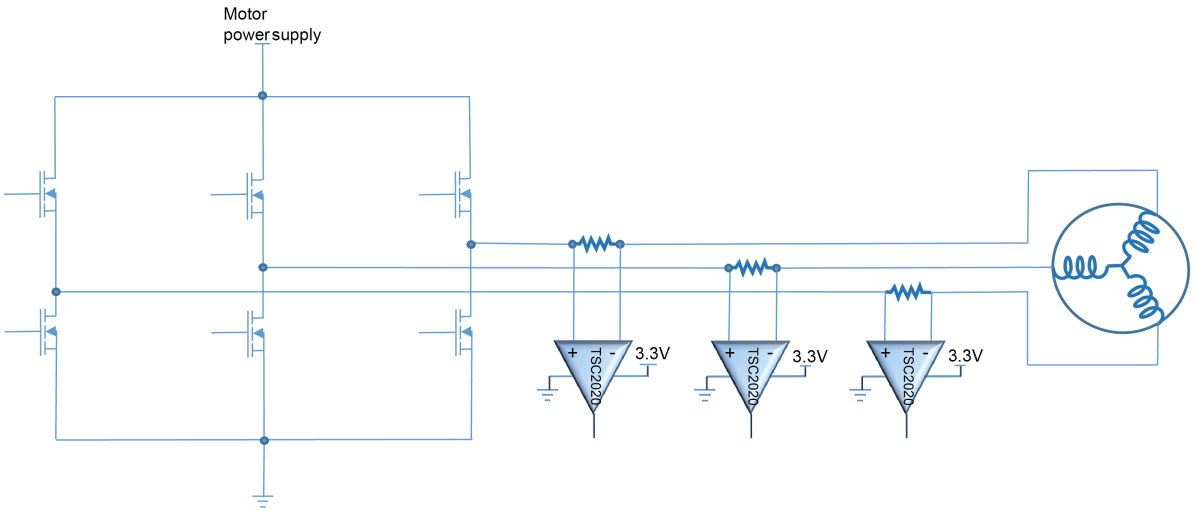

The TSC2020 precision, bidirectional high-side current sensing has been designed specifically for inline current sensing. It features an embedded circuit for enhanced PWM rejection as well as a zero drift precision architecture which makes it the preferred choice for such a configuration.

This topology can only be used with vector control and it is mainly for high-end motor control requiring precise current phase measurement, as is the case for electric power steering or eTurbo application.

The main advantage of this topology is that the current can be read without a strong linkage to the PWM status and without timing limitations in case of very small PWM applied to the phase (whereas low-side current sensing can only be executed while the low-side transistor of that leg is on).

It also allows the detection of phase short-circuits.

2 The TSC2020 in BDLC motor application: inline phase current topology

The TSC2020 provides an extended input common range from -4 V below the negative supply voltage, and up to 100 V, allowing either low-side or high-side current sensing, while the TSC2020 devices can operate from 2.7 to 5.5 V. In addition, the TSC2020 has been specially designed to support fast common-mode voltage variation and offers good accuracy, in order to provide a current picture as close as possible to reality.

2.1 The application description

The motor control system can be depicted in four main blocks (see Figure 8).

Figure 8. Overall system architecture

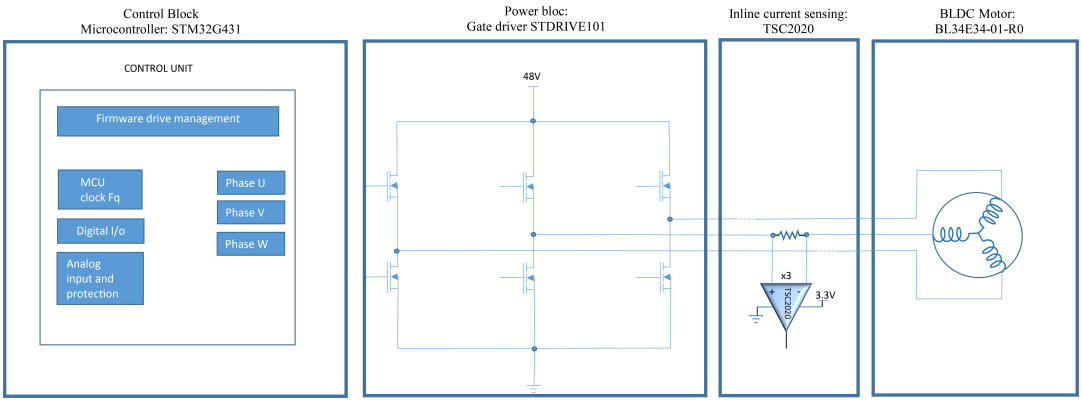

Control block: Its main task is to accept user commands and drive a motor. The STM32G431 microcontroller provides all digital signals to properly implement motor driver control.

Power block: Based on the STDRIVE101, a three-phase gate driver, and the STL110N10F7 power MOSFETs.

Motor: The motor used in this application is a three-phase BLDC motor, BL34E34-01-R0, powered with 48 V.

Shunt + inline current sensing: A shunt of 10 mΩ with a 1% accuracy has been used as well as a TSC2020 current sensing in order to measure the current in one phase of the motor.

The ST evaluation board EVAL STDRIVE101 is combined with the Nucleo board NUCLEO-G431RB.

The purpose of this setup is to demonstrate the TSC2020 performance in motor application control, and not to develop the full algorithm.

It provides an affordable and easy-to-use solution for driving three-phase brushless DC motors.

To measure the current, the STEVAL-AETKT4V1 evaluation board with a TSC2020 current sensing (gain 20) and a shunt of 10 mΩ has been used.

More information about this Nucleo kit, and the TSC2020 evaluation board STEVAL-AETKT4V1 are available on the ST website.

Figure 9. Application system

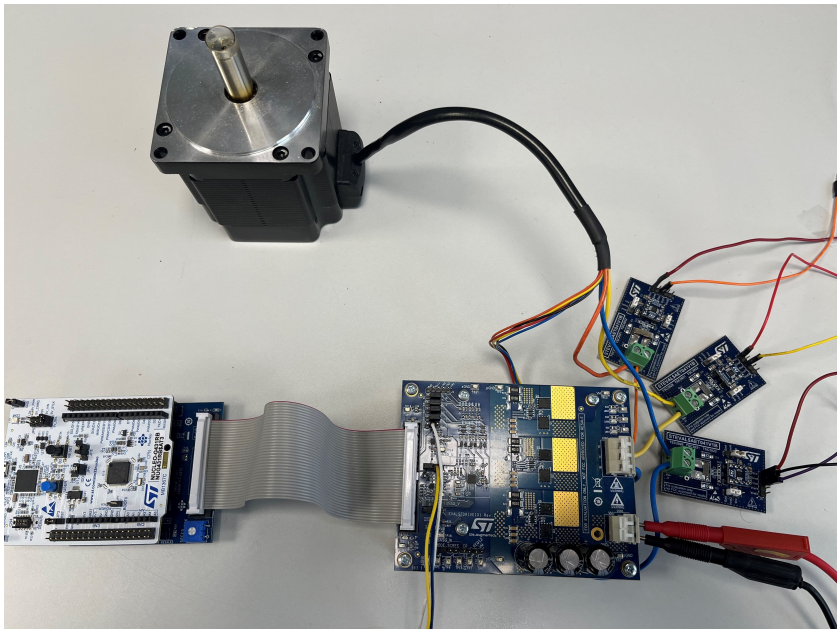

Component choice:

2.1.1 Shunt resistor

The selection of the shunt resistor is a tradeoff between dynamic range and power dissipation.

Generally, in high-current sensing applications, the focus is to reduce as much as possible the power dissipation (I^2R) by choosing the smallest shunt value.

The full-scale current range (Imax-Imin) defines the shunt value based on the full output voltage range and the gain of the TSC2020. The TSC2020 offers the possibility to work with full-scale ΔVout = 100 mV to Vcc -100 mV with a maximum gain accuracy of 0.3%.

To first order, the full current range to measure through Rsense can be defined by Equation 1, accounting for gain error and input offset voltage as inaccuracy parameters:

$$Isense_{full_{scale}} * Rshunt = \frac{Vcc - 200mV}{TSC_{Gain(1+Eg)}} - 2 * |Vio| \quad (1)$$

The Vref voltage should be set such that the output is at Vcc/2 when the sensed current is at (Imin + Imax)/2. This means that Vref=Vcc/2-TSCgain*Rshunt*(Imin+Imax)/2. In this typical application, the TSC2020 is supplied with 3.3 V and the maximum current that the BLDC motor can deliver is 7.2 A. The TSC2020 will be used in bidirectional mode with a Vref set to 1.65 V, so the shunt value can be set to 10 mΩ.

Note that Vref accuracy has not been taken into account in Equation 1. If it is 10 mV, then an extra 2 * 10 mV = 20 mV should be considered for the full-scale calculation (consider 220 mV instead of 200 mV).

2.1.2 Output RC

The demonstrated example circuit uses the built-in 12-bit SAR ADC of the STM32G431 for data acquisition. It is recommended to place an RC filter at the input of any SAR ADC to limit the effect of kickback injection from the internal sample-and-hold capacitor onto the ADC input pin. If, before a sampling, this capacitance is fully discharged, a fast and large current load can appear at the output of the TSC2020 during the sample-and-hold phase. The effect of the ADC sample-and-hold can be effectively smoothed by an RC filter on the TSC2020 output as suggested by the schematic below (Figure 10). The capacitor of the external filter must be chosen much higher than the internal ADC capacitor, in order to easily absorb the sudden voltage variation at the output due to the ADC's sample-and-hold operation. The resistance must be chosen according to the application speed of the system in order not to impact the whole application.

In this case, the internal sample-and-hold capacitance of the integrated 12-bit SAR ADC of STM32G431 is 5 pF typically. We generally suggest using an external kickback capacitance at least five times higher than the internal sample-and-hold capacitance. In our typical application, a 100 pF will be chosen to limit the kickback effect as much as possible, and ensure a recovery time that is as fast as possible. The TSC2020 can support 100 pF on its output without any stability issue. Nevertheless, we will add a series resistance of 10 Ω in order to fix the RC constant value.

Figure 10. The TSC2020 configuration

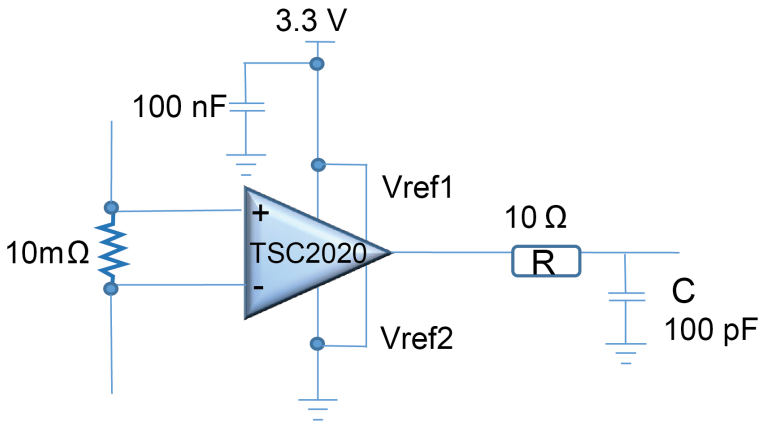

Nevertheless, if the characteristics of the ADC used are different in terms of precision and speed, it may require a higher kickback capacitance. In this case, the series resistance will be even more important, as it will serve as isolation to ensure proper stability of the TSC2020.

Figure 11 shows the minimum series resistors that must be added to the output to make a system stable.

Figure 11. Stability criteria with a series resistor

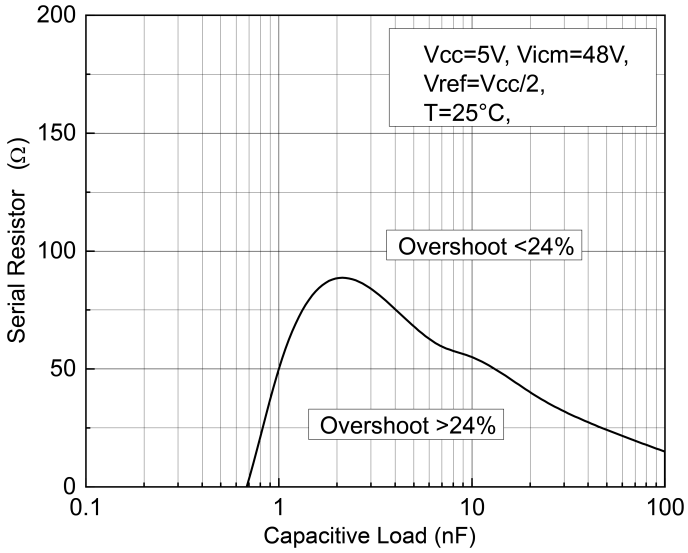

2.2 Theoretical expected error calculation

The principal sources of error that can occur at the output of the TSC2020 are mainly due to input offset voltage, gain error and common-mode rejection ratio. In addition, the shunt resistance accuracy should be taken into account. The simplest way to estimate the total error at the output of the current sensing on the current measurement is to sum up all the imperfections caused by the current sensing and its external environment such as the shunt and the voltage reference. This approach is very pessimistic, and the chance to get all the maximum parameter values on a same die is extremely low. In order to have a good idea of the maximum possible error on the output, we can use a simplified statistical method, but with approximation errors. Total error can be determined by using the root-sum-of-the-squares (RSS), a method to combine the error terms in a quadratic sum. Statistical error on the output based on RSS approximation can be described as in Equation 2:

$$error\ Rss = \sqrt{\begin{aligned}&(\varepsilon G)^2 + \left(\frac{dG}{dT} * \Delta T\right)^2 + (\varepsilon shunt)^2 + \left(\varepsilon shunt_{tempco} * \Delta T\right)^2 + \left(\frac{Vio}{Rshunt.I}\right)^2 + \left(\frac{\left(\frac{dVio}{dT}\right) * \Delta T}{Rshunt.I}\right)^2 \\ &+ \left(\frac{Vcc_{Ds} - Vcc_{Sys}}{\frac{SVR}{Rshunt.I}}\right)^2 + \left(\frac{Vicm_{Ds} - Vicm_{Sys}}{\frac{CMRR}{Rshunt.I}}\right)^2 + \left(\frac{Vref.(\varepsilon ref)}{G.Rshunt.I}\right)^2\end{aligned}} \quad (2)$$

Error is defined as output offset divided by Gain x Vsense. In this typical application, the input common voltage varies between ground and 48 V (PWM driving the BLDC motor). From the above Equation 2, when the input common voltage is 48 V, the error due to the CMRR is null. But when Vicm = 0 V, the CMRR error must be taken into account to express the output voltage.

Note that the input bias currents are not taken into account in Equation 2.

The linearity represents 0.01% of error only. Therefore,in this calculation, it is omitted because it is negligible.

Here is a table summarizing all the expected error terms using the TSC2020.

Table 1. Output voltage error @ 25 °C

Error source	Calculus	Output voltage error
Gain error	20*Vsense*0.3%	20*Vsense*0.3%
Vio error	20*400 µV	8 mV
CMRR error for Vicm = 48 V	$20*\frac{48V - 48V}{\frac{100}{10^{\frac{}{20}}}}$	0
CMRR error for Vicm = 0 V	$20*\frac{48V - 0V}{\frac{100}{10^{\frac{}{20}}}}$	9.6 mV
SVR	$20*\frac{5V - 3.3V}{\frac{100}{10^{\frac{}{20}}}}$	340 µV
Vocm error	1.65*0.1%	1.65 mV
Shunt resistor	20*Vsense*1%	20*Vsense*1%

Let's consider the expected error on the TSC2020 output for a current to sense of 1 A. Theoretically, if we consider an ideal current sensing and shunt, the output voltage should be 1 A * 10 mΩ * 20 = 200 mV above Vref. But as a perfect world doesn't exist, at least in the semiconductor industry, we can add all the errors listed above to the expected output value, linked to the TSC2020 and shunt used.

For a Vicm = 48 V and at a temperature T = 25 °C, the expected error on TSC2020 output is defined by Equation 3:

$$error\ Rss = \sqrt{600\mu V^2 + 8mV^2 + 340\mu V^2 + 1.65mV^2 + 2mV^2} = 8.44mV \quad (3)$$

It represents an error of 4.2% for a current sense of 1 A.

Both Figure 12 and Figure 13 express the expected error in the output versus the current flowing into the motor phase. These curves are a graphical representation of the Equation 2, where the input voltage offset, the input offset voltage drift, the gain error, the CMRR and SVR error, the output common-mode voltage error, and the accuracy of the shunt resistance are involved.

The Figure 12 and Figure 13 represent the total error in % on the output at ambient and 125 °C, for Vicm = 48 V and Vicm = 0 V, by using a shunt of 10 mΩ at 1% and a current flowing into one motor phase in the range of [0.2 to 7.2 A].

Note that Vref is set to Vcc/2, the current from 0.2 A to 7.2 A has been plotted only. The symmetrical graphs would apply for negative current.

Figure 12. Total error vs current @ Vicm = 48 V

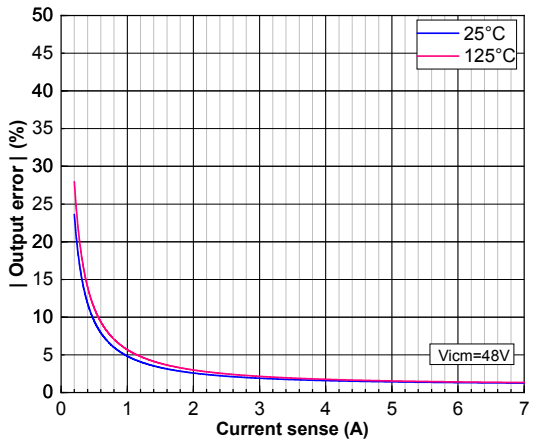

Figure 13. Total error vs current @ Vicm = 0 V

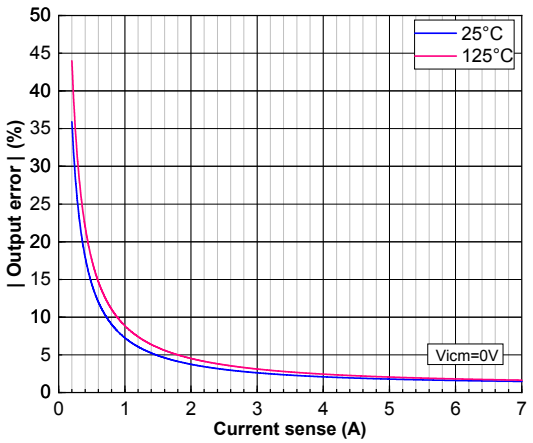

2.3 Fast common-mode rejection

Inline phase sensing provides accurate motor phase-current measurement, enhancing the quality of data for the motor-control processing. The system processor can determine the current in each phase of the three-phase motor at any moment, leading to more efficient motor operation. One of the biggest challenges is to deal with fast and large variations of the common-mode voltage of the PWM signal, which can perturb the output signal. The main difficulties for an inline current sensing is to be able to treat a small differential signal while rejecting a large common-mode signal.

The PWM input signal acts as a fast transient on the input and as a strong and instantaneous perturbation of the input bias of the devices, which impact the recovery time on the output. This recovery time must be as low as possible to guarantee the best signal integrity.

The TSC2020 has been specially designed to ensure a quick settling time and high accuracy in response to a fast common input transition, and allows minimization of the PWM duty cycle.

Figure 14 shows that the output requires less than 4 µs to recover after a common-mode step variation of 48 V.

Figure 14. 48 V common-mode step response

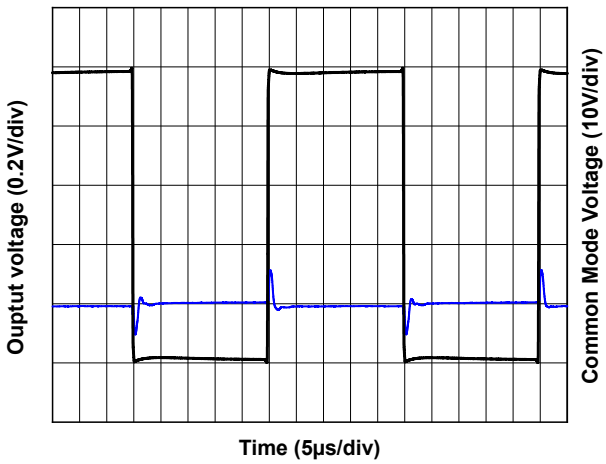

2.4 The TSC2020 in motor application

The Figure 15 shows the response of the TSC2020 in the application described by Figure 7.

Only one phase out of three has been measured.

The PWM frequency of the motor is 16 kHz, represented by the purple curve in Figure 15.

The green curve comes from a current probe placed on the same phase as the shunt resistance. The red curve represents the output of the TSC2020 and shows its good signal integrity. The red and green curves can be superposed, so the TSC2020 provides an accurate signal for the motor control.

On the fast transition of the current, a response time of less than 4 µs can be observed, due to the TSC2020 response time to a fast common-mode transition.

Figure 15. Behavior of the output of the TSC2020 in a motor application

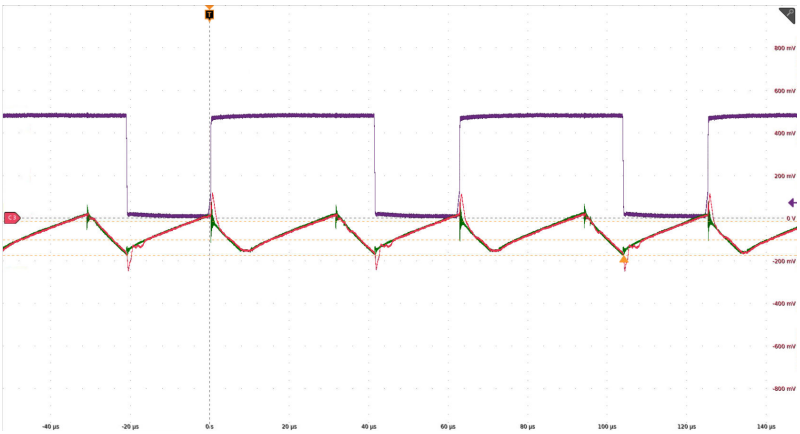

2.5 Comparison of low-side and inline current sensing

This section compares low-side and inline phase current sensing. The introduced motor control board EVAL_STDRIVE101 uses a low-side current sensing approach based on TSV991. The test has been done as described in Figure 16, by comparing the output of the TSC2020 and the TSV991, which represents the voltage information about the current Ibc flowing into the motor.

Figure 16. Comparison of low-side and inline current sensing

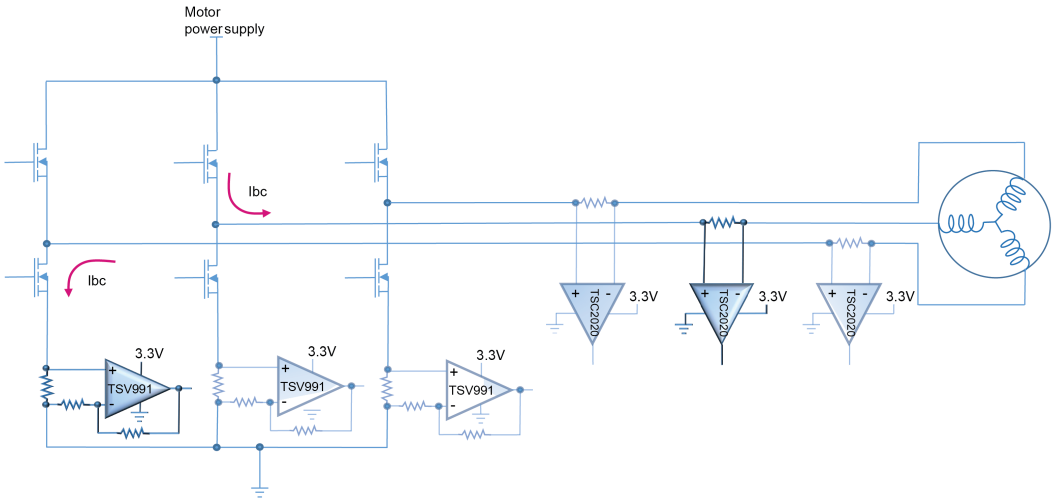

In the low-side current sensing approach, developed with the TSV991 op amp, the sampling of the currents must be performed when the corresponding low-side switch is turned on, as indicated in Figure 17 when PWM = 0 V.

When PWM = 48 V, no information about the current flowing into a phase motor can be fed back with low-side current sensing. This is why in low-side current sensing, a complex algorithm must be developed to estimate the current during the high-side phase. In any case, continuous current measurement is not possible with this technique.

The light green curve depicts the probing of the TSV991 output. The information is available only when the low-side transistor is ON. When the high side transistor is ON, the output voltage is close to GND.

Alternatively, with high-side inline configuration, the current measurement can be done during the entire PWM cycle. The output of the inline TSC2020 current sensing in red follows the current flowing into the phase motor (dark green curve monitored by a current probe). With this technique, continuous current measurement is possible, allowing for a lighter algorithm and a better drive of the motor improving the efficiency at the same time.

Figure 17. Comparison of low-side and high-side inline current phase

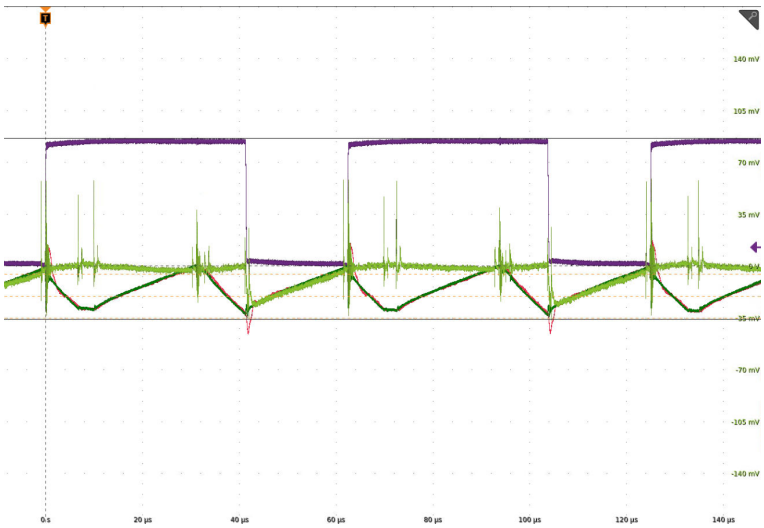

3 Conclusion

In motor control applications, the measurement of the current is fundamental to provide feedback to the motor. Several topologies can be used to develop this current sensing, with pros and cons.

A low-side approach can be easily developed using the TSV991 (gain > 4), with the advantage of an easy implementation and a cheaper solution.

For improved precision, you may prefer to choose the TSV771 series.

In some automotive applications, the motor is directly mounted on the chassis of the car. In this case, there is no possibility to insert a shunt between the motor and ground, and so it is not possible to use a low-side current sensing topology.

In this case, a high-side current sensing could be the solution, as it is less intrusive than low-side current sensing. If an accurate measurement of the phase current is critical, as for example for electric power steering applications or applications where functional safety is a must, inline current sensing can be a very good solution.

It allows for sensing the current continuously with good precision and fast response time, which is ideal to improve motor control efficiency and lighten processing information.

The TSC2020, a bidirectional current sensing, offers a wide common range and is therefore a good choice for these kinds of applications, due to its good response time to a fast step variation on the input common-mode voltage and its good accuracy.

Revision history

Table 2. **Document revision history**

Date	Version	Changes
23-Sep-2025	1	Initial release.

Contents

List of tables

List of figures

IMPORTANT NOTICE – READ CAREFULLY

STMicroelectronics NV and its subsidiaries (“ST”) reserve the right to make changes, corrections, enhancements, modifications, and improvements to ST products and/or to this document at any time without notice.

In the event of any conflict between the provisions of this document and the provisions of any contractual arrangement in force between the purchasers and ST, the provisions of such contractual arrangement shall prevail.

The purchasers should obtain the latest relevant information on ST products before placing orders. ST products are sold pursuant to ST’s terms and conditions of sale in place at the time of order acknowledgment.

The purchasers are solely responsible for the choice, selection, and use of ST products and ST assumes no liability for application assistance or the design of the purchasers’ products.

No license, express or implied, to any intellectual property right is granted by ST herein.

Resale of ST products with provisions different from the information set forth herein shall void any warranty granted by ST for such product.

If the purchasers identify an ST product that meets their functional and performance requirements but that is not designated for the purchasers' market segment, the purchasers shall contact ST for more information.

ST and the ST logo are trademarks of ST. For additional information about ST trademarks, refer to www.st.com/trademarks. All other product or service names are the property of their respective owners.

Information in this document supersedes and replaces information previously supplied in any prior versions of this document.